

Crystal packing

There are no short intermolecular contacts less than the sum of the van der Waals radii.

The programs used are: *DEVIN* (Riche, 1972); *ORTEP* (Johnson, 1965); the *NRC* series (Ahmed, Hall, Pippy & Huber, 1966); and *ORFLS* (Busing, Martin & Levy, 1962).

The authors wish to thank Dr Eitelman for supplying the crystals and Professor Horton for helpful discussions.

References

- AHMED, F. R., HALL, S. R., PIPPY, M. E. & HUBER, C. P. (1966). *NRC* programs. *World List of Crystallographic Computer Programs*. 2nd ed., p. 52. Utrecht: Oosthoek.
- ALTONA, C., GEISE, H. J. & ROMERS, C. (1968). *Tetrahedron*, **24**, 13–32.
- BLACKWOOD, J. E., GLADYS, C. L., LOENING, K. L., PETRARCA, A. E. & RUSH, J. E. (1968). *J. Amer. Chem. Soc.* **90**, 509–510.
- BUSING, W. R., MARTIN, K. O. & LEVY, H. A. (1962). *ORFLS*. Oak Ridge National Laboratory Report ORNL-TM-305.
- DOYLE, P. A. & TURNER, P. S. (1968). *Acta Cryst.* **A24**, 390–397.
- DUCRUIX, A. & PASCARD-BILLY, C. (1974). *Acta Cryst.* **B30**, 1056–1063.
- DUCRUIX, A. & PASCARD-BILLY, C. (1975a). *Acta Cryst.* **B31**, 2250–2256.
- DUCRUIX, A. & PASCARD-BILLY, C. (1975b). *Acta Cryst.* **A31**, S108.
- DUCRUIX, A. & PASCARD-BILLY, C. (1977). To be published.
- HUNTER, F. D. & ROSENSTEIN, R. D. (1968). *Acta Cryst.* **B24**, 1652–1660.
- JOHNSON, C. K. (1965). *ORTEP*. Oak Ridge National Laboratory Report ORNL-3794.
- KIM, H. S. & JEFFREY, G. A. (1969). *Acta Cryst.* **B25**, 2607–2613.
- RICHE, C. (1972). *DEVIN*. Institut de Chimie des Substances Naturelles Rapport n° 1.
- RICHE, C. (1973). *Acta Cryst.* **A29**, 133–137.
- STEWART, R. F., DAVIDSON, E. R. & SIMPSON, W. T. (1965). *J. Chem. Phys.* **42**, 3175–3187.

Acta Cryst. (1977). **B33**, 1389–1396

On the Crystal Structure of LiTe_3 *

BY DIANE Y. VALENTINE,† O. BURL CAVIN‡ AND HARRY L. YAKEL‡
Oak Ridge National Laboratory, Oak Ridge, Tennessee 37830, USA

(Received 2 July 1976; accepted 20 October 1976)

The crystal structure of LiTe_3 has been analyzed from X-ray and neutron powder diffraction data, and from photographically recorded X-ray single-crystal data. The proposed structure is based on harmonically related positional displacements of Te atoms from a reference structure that has six Te atoms at the centers of faces and edges of a cubic unit cell. The rhombohedrally centered hexagonal cell corresponding to the diffraction symmetry has $|A| = 8.7144$ (3) and $|C| = 5.3363$ (2) Å. Displacements are in basal-plane directions of this hexagonal cell; the wave vector of the harmonic function describing them is parallel to C and has a period of $4|C|$ from -103 to 150°C . The unique axial ratio ($\equiv\sqrt{\frac{3}{2}}$) of the hexagonal cell of the reference structure is also maintained over this temperature range. While the actual structure must be classified as a superstructure, the symmetry relationships developed for modulated three-dimensional structure (MS_3) groups are applicable to its derivation. The proposed displacements produce sections normal to C in which segments of Te-like chains can be distinguished. These sections are separated by metal-like layers that occur as the displacements become small. Li atoms are regularly distributed in channels parallel to C.

Introduction

Lithium tritelluride is the only phase of unknown structure in the Li–Te system. We prepared LiTe_3 in an in-

vestigation of materials that might be produced in a molten-salt breeder reactor. This compound, first reported by Foster, Johnson, Davis, Peck & Schablaske (1969), then confirmed by Cunningham, Johnson & Cairns (1973), melts congruently at 460°C and forms simple eutectics with Te at 423°C and with Li_2Te (fluorite structure, Zintl, Harder & Dauth, 1934) at 449°C . Cunningham *et al.* (1973) stated that X-ray powder patterns of LiTe_3 were consistent with a body-

* Research sponsored by the Energy Research and Development Administration under contract with the Union Carbide Corporation.

† Chemistry Division.

‡ Metals and Ceramics Division.

centered-cubic structure with $a = 6.162 \text{ \AA}$; the nature of that structure was not specified. In this paper, we present a more detailed description of the X-ray diffraction data and show that applications of modulated symmetry theories to the problem yield a structure with only one variable parameter whose value may be fixed by qualitative comparisons of predicted and observed intensities.

Experimental

The Te purity (99.999 wt% Te, Alpha Ventron Products, Danvers, Massachusetts) was verified by spectroscopic analysis. Li (Foote Mineral Company, Philadelphia, Pennsylvania) was purified by exposure to Zr at 800°C , and as recast contained 6 ppm nitrogen and 183 ppm oxygen. LiTe_3 was synthesized from Te and Li_2Te by grinding and mixing appropriate weights of each in a dry box (~ 1 ppm O_2 and < 1 ppm H_2O) and placing the mixture in an out-gassed quartz bulb. The bulb was evacuated to $5 \mu\text{m Hg}$, sealed, heated at 550°C for 1 h, and finally furnace-cooled. All subsequent operations were carried out in argon- or helium-filled dry boxes to prevent rapid reaction in air. Chemical analyses gave 1.67 ± 0.1 wt% Li, $98.4_4 \pm 0.5$ wt% Te (theoretical values for LiTe_3 are 1.65 wt% Li and 98.35 wt% Te), and 275 ppm oxygen as the major light-element impurity.

X-ray powder diffraction data were obtained from material sealed into 0.3 mm diameter glass capillaries. Single-crystal specimens culled from the crushed material were inserted into 0.1 mm diameter glass capillaries sealed with a hot Pt wire inside the dry box. Room-temperature X-ray diffraction data were recorded photographically with 114.6 mm diameter Debye-Scherrer cameras, and with rotation, oscillation, and Weissenberg single-crystal cameras. High-temperature powder data were observed in a modified Hilger & Watts S.250 camera; low-temperature single-crystal data were recorded with an Enraf-Nonius Weissenberg camera. Ni-filtered Cu $K\bar{\alpha}$ X radiation ($\lambda = 1.54178 \text{ \AA}$) was employed for all X-ray diffraction experiments.

A sample for neutron powder diffraction was loaded into a thin-walled 0.95 cm diameter Al tube sealed by a Pb gasket. Data were recorded with a relatively low-resolution powder diffractometer (HB-3) at the High-Flux Isotope Reactor at a wavelength of 1.542 \AA .

Results

Well exposed room-temperature [$t = 21 (1)^\circ\text{C}$] powder patterns gave no evidence for either Te or Li_2Te . The prominent (or main) reflections were rigorously consistent with the 6.162 \AA body-centered-cubic lattice

Table 1. Cu $K\bar{\alpha}$ X-ray powder diffraction data for LiTe_3 at $t = 21 \pm 1^\circ\text{C}$ ^(a)

<i>HKLM</i>	d_{calc} (Å)	d_{obs} (Å)	$I_{\text{obs}}^{(b)}$
11.00, 10.10	4.357	4.324	25
02.10	3.081	3.060	74
30.00, 21.10, 01.20	2.512	2.504	21
22.00, 20.20	2.179	2.170	94
13.1 $\bar{1}$	2.008	1.999	4
13.10, 12.20	1.949	1.942	13
13.11	1.879	1.876	4
40.10, 00.40	1.779	1.775	38
31.2 $\bar{1}$	1.726	1.721	3
41.00, 32.10,	1.647	1.643	28
31.20, 11.30			
31.21	1.569	1.565	3
04.20	1.541	1.537	31
33.00, 05.10,	1.452	1.449	15
23.20, 30.30			
24.10, 22.30	1.378	1.376	100
51.1 $\bar{1}$	1.332	1.329	4
51.10, 50.20, 10.40	1.314	1.312	13
51.11	1.292	1.291	4
60.00, 42.20, 02.40	1.258	1.257	46
⋮	⋮	⋮	⋮
35.42, 72.21	0.85935	0.85914	6
46.10, 42.50	0.85452	0.85415	62
		0.85414	31
18.2 $\bar{1}$, 16.41	0.84842	0.84842	9
		0.84824	4
73.1 $\bar{1}$	0.84311	0.84290	8
		0.84268	4
18.20, 90.00, 73.10,	0.83854	0.83837	21
63.30, 35.40, 70.40,		0.83833	11
15.50, 30.60			
73.11, 34.5 $\bar{1}$	0.83278	0.83255	8
		0.83275	4
18.21	0.82776	0.82744	5
		0.82735	2
82.00, 64.20,	0.82343	0.82322	93
62.40, 22.60		0.82328	46
35.41, 37.2 $\bar{1}$	0.81797	0.81783	12
		0.81799	6
15.51	0.81321	0.81316	4
37.20, 34.50	0.80911	0.80898	15
		0.80895	7
61.5 $\bar{1}$	0.80393	0.80387	4
		0.80395	2
37.21, 54.1 $\bar{1}$	0.79941	0.79946	10
		0.79953	5
55.31	0.79496	0.79498	12
		0.79511	6
19.1 $\bar{1}$, 65.1 $\bar{1}$, 34.5 $\bar{1}$	0.78628	0.78632	18
		0.78638	
19.10, 74.00, 65.10,	0.78258	0.78258	44
55.30, 54.40,		0.78254	22
61.50, 14.60			
19.11, 65.11	0.77789	0.77797	25
		0.77796	14

(a) A complete version of this table has been filed with the ASTM Joint Committee on Powder Diffraction Standards.

(b) Observed intensities were estimated from densitometer scans of a well exposed Debye-Scherrer pattern of LiTe_3 . They have not been corrected for absorption or Lorentz-polarization effects.

reported by Cunningham *et al.* (1973). Corrected for differences in multiplicity, main reflections with all cubic indices even were systematically more intense than those with two indices odd. No splitting or broadening of these sharp main reflections was observed. In addition, we noted a second series of sharp (satellite) reflections whose intensities, vanishingly weak at low Bragg angles, increased with scattering angle and became comparable to main-reflection intensities as 2θ approached 180° . Bragg spacings and intensities from a powder pattern are listed in Table 1.

To date, all of the small objects, culled from the reaction product as possible crystals, have indeed proved to be single crystals. The significance of this observation is that X-ray diffraction data from the crystals at room-temperature show only pseudocubic character, even within the set of main reflections. The Laue symmetry of the main reflections approximates $m\bar{3}m$ but is actually $\bar{3}m$. The $[111]$ direction of the cubic pseudocell corresponding to the $\bar{3}$ axis of the true rhombohedral unit cell is the only direction in reciprocal space along which satellite reflections occur.

Vector equations relating the body-centered-cubic pseudocell (small letters) and the rhombohedrally centered hexagonal cell (capital letters) that correctly represents the main reflection Laue symmetry are $\mathbf{A} = \mathbf{a}_1 - \mathbf{a}_3$, $\mathbf{A}_2 = -\mathbf{a}_1 + \mathbf{a}_2$, $\mathbf{C} = \frac{1}{2}(\mathbf{a}_1 + \mathbf{a}_2 + \mathbf{a}_3)$. Since $|\mathbf{a}_i| = 6.1620(2) \text{ \AA}$ at $t = 21^\circ\text{C}$, it follows that $|\mathbf{A}_i| = 8.7144(3) \text{ \AA}$ and $|\mathbf{C}| = 5.3364(2) \text{ \AA}$, with an axial ratio of $0.61237(4) (\equiv \sqrt{\frac{3}{8}}$ within experimental error). If it is assumed that the cubic pseudocell contains two formula weights of LiTe_3 , the X-ray density is $5.532(1) \text{ g cm}^{-3}$; Cunningham *et al.* (1973) gave a density of $5.29(25) \text{ g cm}^{-3}$ measured with an air-comparison pycnometer.

Room-temperature single-crystal diffraction data proved that satellite reflections only occur with indices $HK(L \pm Mk_3)$, where $HK.L$ is an allowed index triple of the rhombohedrally centered hexagonal cell. The order of the satellite is denoted by M , and $k_3 = 0.25(1)$ at $t = 21^\circ\text{C}$. The following statements summarize our qualitative observations of relative satellite intensities from single-crystal data. The Laue symmetry of the satellite reflections is $\bar{3}m$. For a given $HK.L$, pairs of satellites with equal M have nearly equal intensities. Satellites with $M = 1$ have the greatest intensity and are responsible for all non-main reflections observed in the X-ray powder data (see Table 1). Satellites with $M = 2$ are extremely weak but can be seen on over-exposed oscillation patterns; no higher orders have been detected. Relative to the intensity of their neighboring main reflections, the intensity of satellites with common HK decreases with increasing L ; the intensity of those with common L increased with increasing HK . First-order satellites are absent if H or K is 0; otherwise they are most intense if H and K are odd, less intense if H or K is even, and weak if H and K are even.

We attempted to vary k_3 by changing composition and temperature. A sample of LiTe_3 was mixed with enough Te to give an overall composition of 18 at.% Li. The specimen was melted at 550°C in an evacuated quartz bulb, held at 430°C for about 96 h, and furnace-cooled. An X-ray powder pattern showed broad Te reflections and sharp, unsplit reflections of LiTe_3 which gave $|\mathbf{a}_i| = 6.1620(2) \text{ \AA}$, and $k_3 = 0.25(1)$. X-ray powder patterns of pure LiTe_3 were also taken at 150 and 250°C . The 150°C pattern con-

Table 2. Observed and calculated neutron diffraction data for main reflections of LiTe_3^*

<i>HKLM</i>	<i>I</i> _{obs.}	<i>I</i> ₁
11.00, 10.10	8.28	9.46
02.10	8.39	7.86
30.00, 21.10, 01.20	5.66	5.73
22.00, 20.20	7.52	7.29
13.10, 12.20	3.11	3.41
40.10, 00.30	3.38	3.01
31.00, 32.10,	4.46	4.46
31.20, 11.30		
04.20	2.02	1.58
33.00, 05.10,	2.12	2.30
23.20, 03.30		
24.10, 22.30	5.83	4.72
51.10, 50.20, 10.40	1.01	1.31
60.00, 42.20, 02.40	4.36	3.70
52.20, 43.10, 15.20,	2.57	2.98
14.30, 21.40		
61.20, 34.20,	1.73	1.80
33.30, 13.40		
44.00, 40.40,	1.82	1.30
34.21, 32.41†		
70.10, 35.10, 61.20,	0.95	1.49
32.40, 01.50		
62.10, 60.30, 20.50,	3.22	2.75
61.21		
71.00, 53.20, 07.20,	1.42	1.83
52.30, 05.40, 12.50		
26.20, 24.40,	2.24	2.00
53.21, 51.41		
54.10, 63.00,	0.89	1.09
51.40, 31.50		
08.10, 44.30, 04.50	1.98	1.66
<i>R</i> (as defined in text)‡		12%

* Intensities were computed from Te positions given in Table 3 plus Model 1 (*I*₁): Li positions as given in Table 3

Model 2: 4 Li in 4(c); 0,0,z; etc.; $z = \frac{1}{8}$

4 Li in 4(d); $\frac{1}{3}, \frac{2}{3}, z$; etc.; $z = \frac{1}{24}$

4 Li in 4(d); $\frac{1}{3}, \frac{2}{3}, z$; etc.; $z = \frac{7}{24}$

Model 3: 2 Li in 2(b); 0,0,0; 0,0, $\frac{1}{2}$

2 Li in 2(a); 0,0, $\frac{1}{4}$; 0,0, $\frac{3}{4}$

4 Li in 4(d); $\frac{1}{3}, \frac{2}{3}, z$; etc.; $z = 0$

4 Li in 4(d); $\frac{1}{3}, \frac{2}{3}, z$; etc.; $z = \frac{1}{4}$

Model 4: 2 Li in 2(b); 0,0,0; 0,0, $\frac{1}{2}$

4 Li in 4(d); $\frac{1}{3}, \frac{2}{3}, 2z$; etc.; $z = 0$.

All positions are referred to space group $P\bar{3}c1$.

† Main reflections between 90 and 115° (2θ) were broad enough that their intensity distributions occasionally overlapped nearby satellite positions. In such cases, observed intensities were assumed to comprise the sum of main and overlapped satellite reflection intensities.

‡ *R* (model 2) = 21%; *R* (model 3) = 30%; *R* (model 4) = 40%.

tained only the sharp, unsplit main and satellite reflections associated with LiTe_3 ; measurements gave $|\mathbf{a}_i| = 6.1818(4) \text{ \AA}$ and $k_3 = 0.24(2)$. The powder pattern at 250°C indicated partial decomposition of the sample and was not measured. A single crystal of LiTe_3 was cooled to $-103 \pm 5^\circ\text{C}$ and portions of oscillation patterns were recorded. No evidence for a phase transition was observed; spacing measurements gave $|\mathbf{a}_i| = 6.144(5) \text{ \AA}$, $k_3 = 0.24(1)$.

The neutron data from LiTe_3 were of low resolution and only main reflections could be observed above background. A list of these reflections (together with their relative intensities expressed as the product of peak height and width) appears in Table 2.

A structural interpretation of the diffraction data

Neglecting satellites and departures from $m3m$ Laue symmetry, the systematic alternation of main reflection intensities noted in the X-ray powder (and single-crystal) data suggests that the Te atoms in LiTe_3 must occupy positions at or near centers of all cubic pseudo-cell edges and faces. Following the formalism of de Wolff (1974), the structure with Te atoms at these centers will be called the reference structure. Such locations yield structure factors proportional to $2f_{\text{Te}}$ if two cubic indices are odd, and to $6f_{\text{Te}}$ if all cubic indices are even.

The increasing intensity of satellite reflections with increasing scattering angle indicates departures from the reference structure not involving chemical order or faulting, but rather resulting from regular displacements of Te atom positions. Chemical order would be unlikely in view of the stoichiometry of the LiTe_3 phase; regular faulting could be discounted in view of the unusual directional properties such faults would require to reproduce the observed satellites.

Since k_3 is $\frac{1}{4}$, one must consider the actual Te atom positions as constituting a superstructure based on the reference structure. The primitive hexagonal supercell with $|\mathbf{A}_i^s| = 8.714 \text{ \AA}$ and $|\mathbf{C}^s| = 21.35 \text{ \AA}$ would contain 36 Te atoms that might be distributed in several possible ways among the positions of $P\bar{3}c1$ (D_{3d}^4), a space group consistent with the observed Laue symmetry and with some of the systematic reflection absences. Te parameters could be found by Fourier techniques, beginning with main reflections whose phases are immediately known and finally including all observed satellite reflections. A solution to the crystal structure of hepta(tetrathiafulvane) pentaiodide, $(\text{TTF})_7\text{I}_5$, by this method has been given by Johnson (1976).

Such a procedure would ignore unique features of the satellite intensities that do not follow from space group symmetry requirements. These features might be more fully exploited by treating the problem in terms of geometrical structure factors that must have signifi-

cant amplitudes only for main and first-order satellite reflections. Such an analysis has been carried out: it leads to a model equivalent to that derived by a second approach to be described below.

This approach recognizes that the special diffraction features produced by the LiTe_3 superstructure are similar to those produced by modulated structures (de Wolff, 1974); we outline our analysis in order to demonstrate the utility of modulated symmetry relationships to the derivation of special kinds of superstructures. Extensive use is made of the four-dimensional methods and notations introduced by de Wolff (1974) and by van Aalst, den Hollander, Peterse & de Wolff (1976).

Though the reference structure should be assigned to space group $Im\bar{3}m$, it will be described in space group $R\bar{3}m$, since this conforms to the $3'm$ Laue symmetry of the main reflections.* Te atoms may occupy positions $9(e)$, $(2/m)$, $(\bar{x} = \frac{1}{4}, \bar{y} = 0, \bar{z} = 0; \text{etc.})$ in this structure. The actual position of a Te atom in a given reference structure cell is then specified by the coordinates $x = \bar{x} + u(\tau)$, $y = \bar{y} + v(\tau)$, $z = \bar{z} + w(\tau)$, where u , v , and w have values that depend on the cell in which the atom is located and are functions of a 'modulation' parameter $\tau = k_3 \bar{z}$. In a first-order harmonic approximation,

$$u(\tau) = U_c \sin(2\pi\tau) + U_s \cos(2\pi\tau),$$

$$v(\tau) = V_c \sin(2\pi\tau) + V_s \cos(2\pi\tau),$$

and

$$w(\tau) = W_c \sin(2\pi\tau) + W_s \cos(2\pi\tau).$$

The crystal system of the MS_3 group in R_4 space is rhombohedral monoclinic (Wondratschek, Bülow & Neubüser, 1971) and the point group is $\bar{3}'m$, where the prime indicates sign reversal in the fourth coordinate of direct space. Since for all observed reflections $HKLM$, $-H + K + L = 3n$, the space group in R_4 is rhombohedrally centered with respect to the x , y and z coordinates. The extinction of odd M satellites in $HO\bar{L}M$ zones is the result of a glide plane whose translational component has the direction of the fourth base vector. The general positions of the resulting space group in R_4 , and the corresponding three-dimensional coordinates, expressed in terms of \bar{x} , \bar{y} , \bar{z} , u , v and w , are listed in the Appendix.

Te atoms must occupy special positions because their multiplicity (9) is lower than 36. Since they project as split atoms lying close to the $2/m$ sites of $R\bar{3}m$ in the reference structure, the strings that represent them in R_4 space must coincide with their glide-plane images.

* If Te positions were determined from main X-ray reflection intensities alone, they would display a split-atom structure with trigonal symmetry. Split atoms would be located close to the $9(e)$ positions of $R\bar{3}m$. The sequential ordering of the positions of these split atoms gives rise to the satellite reflections. Nevertheless, average positions of the nine Te atoms in the rhombohedrally centered hexagonal reference structure cell would be equivalent to the cubic reference structure defined above.

Thus, for atoms near $\bar{x} = \frac{1}{2}, \bar{y} = 0$, the first and the eighth transformations from Table 5(b) in the Appendix give

$$u(\tau) = -u(\tau + \frac{1}{2}),$$

$$v(\tau) = v(\tau + \frac{1}{2}),$$

$$w(\tau) = w(\tau + \frac{1}{2}).$$

If a first-order harmonic approximation is assumed, $V_c = V_s = W_c = W_s = 0$. Furthermore, since $2/m$ sites are centers of symmetry, Te atom positions must be invariant to corresponding operations in R_4 space. With the origin in R_4 as a center through which a Te string passes, and with the first and fourth transformations from Table 5(b) operating on atoms near $\bar{x} = \frac{1}{2}, \bar{y} = 0$,

$$u(\tau) = -u(-\tau).$$

Thus, in the harmonic approximation, $U_s = 0$. The coefficient U_c is then left as the only parameter fixing Te atom positions in the proposed three-dimensional structure.

Given that $k_3 = \frac{1}{4}$, positional parameters of Te atoms

in this superstructure may be written as a function of U_c , and structure factors can be computed in a straightforward manner. Calculations for a range of U_c values show that $U_c = 0.020(2)$ gives good qualitative agree-

Table 3. Atom positional parameters for the proposed structure of LiTe_3 referred to space group $P\bar{3}c1$

Numbers in parentheses following x parameters of Te(2), Te(3) and Te(4) represent errors in the last significant figures of the parameters based on the estimated error in U_c . Parameters followed by asterisks are not fixed by the space group and are not 'modulated'; these values correspond to the fixed parameters of the reference structure.

Position	x	y	z
Te(1) 6(e)	$\frac{1}{2}$	0	0
Te(2) 6(f)	0.520(2)	0	$\frac{1}{4}$
Te(3) 12(g)	0.177(1)	0.3333*	0.0833*
Te(4) 12(g)	-0.149(2)	0.6667*	0.1667*
Li(1) 2(b)	0	0	0
Li(2) 2(a)	0	0	$\frac{1}{4}$
Li(3) 4(d)	$\frac{1}{2}$	$\frac{2}{3}$	0.1667*
Li(4) 4(d)	$\frac{1}{2}$	$\frac{1}{3}$	-0.0833*

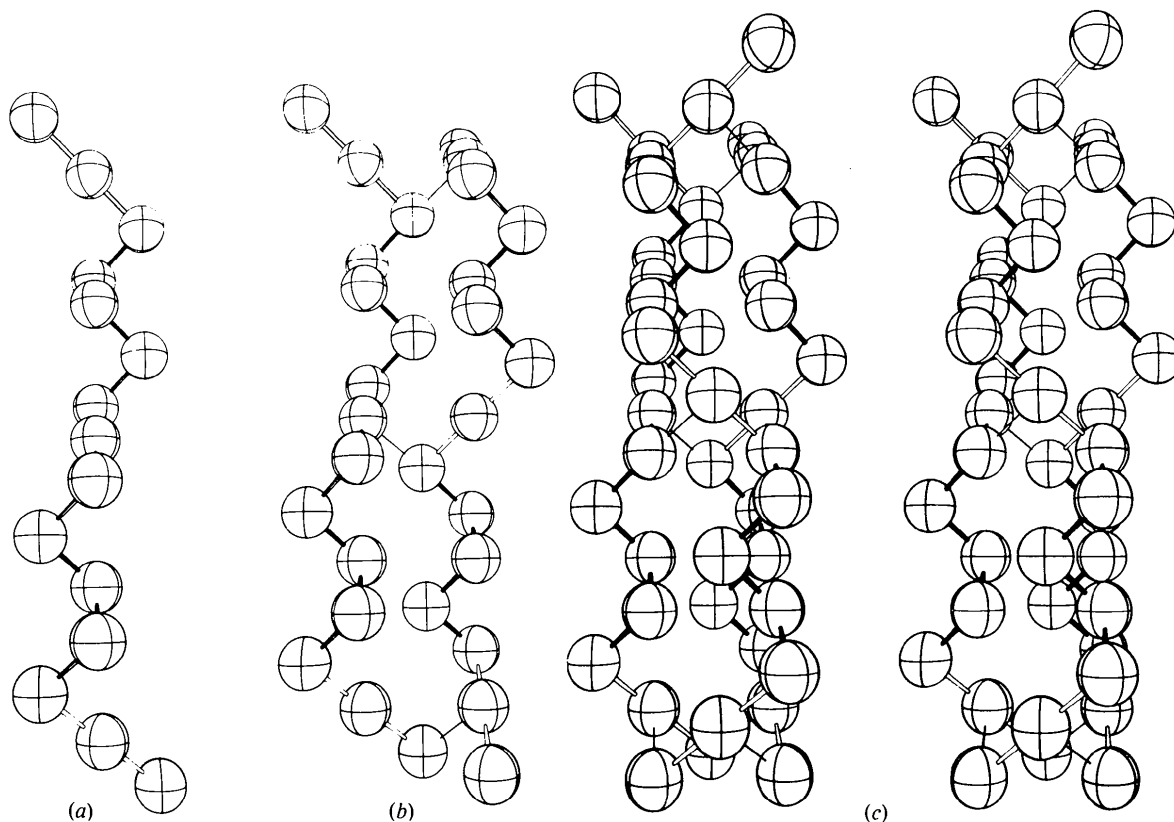


Fig. 1. Views of 'chain-like' Te atom arrangements in the proposed structure of LiTe_3 . The C vector is directed upward and A_2 is directed approximately to the right in the plane of the paper for each drawing. Te atoms are shown with an arbitrary radius of 0.7 \AA . Shortest intra-'chain' Te-Te distances are indicated by solid bonds and the bond shading decreases as the bond distance increases. Shortest inter-'chain' distances are indicated by thin lines. (a) A section of a single 'chain' centred at $x = \frac{1}{2}, y = 0$. (b) The 'chain' in (a) plus the matching section of the 'chain' centred at $\bar{x} = \frac{1}{2}, \bar{y} = \frac{1}{2}$. (c) A stereo view of the 'chains' in (b) plus the matching section of the 'chain' centred at $\bar{x} = 1, \bar{y} = \frac{1}{2}$. Views are centred at $\bar{x} = \frac{1}{2}, \bar{y} = 0, \bar{z} = 2$ for (a), and at $\bar{x} = \frac{1}{2}, \bar{y} = \frac{1}{2}, \bar{z} = 2$ for (b) and (c). Li atoms are not shown.

Table 4. Some prominent interatomic distances (Å) and angles ($^\circ$) in the proposed structure of LiTe_3

Values of N are the number of equivalent distances about the first atom specified. Primes indicate atoms in 'chains' other than those in which the first atom (distances) or central atom (angles) specified is located. Numbers in parentheses following distances and angles represent errors in the last significant figures of the given values based on the estimated error in U_c and the experimental errors in the lattice parameters.

Intra-'chain' distances			Intra-'chain' angles		
N					
2	Te(1)—Te(3)	3.02 (1)	Te(3)—Te(1)—Te(3)	180.0	
1	Te(3)—Te(4)	2.92 (1)	Te(4)—Te(3)—Te(1)	92.4 (2)	
1	Te(4)—Te(2)	2.86 (1)	Te(2)—Te(4)—Te(3)	94.3 (4)	
			Te(4)—Te(2)—Te(4)	95.0 (5)	
Inter-'chain' distances			Li—Te distances		
N			N		
2	Te(1)—Te(3)'	3.14 (1)	6	Li(1)—Te(3)	3.082 (2)
1	Te(3)—Te(4)'	3.25 (1)	6	Li(2)—Te(4)	3.085 (2)
1	Te(4)—Te(2)'	3.32 (2)	3	Li(3)—Te(3)	3.082 (2)
			3	Li(3)—Te(2)	3.086 (2)
			3	Li(4)—Te(1)	3.081 (2)
			3	Li(4)—Te(4)	3.085 (2)

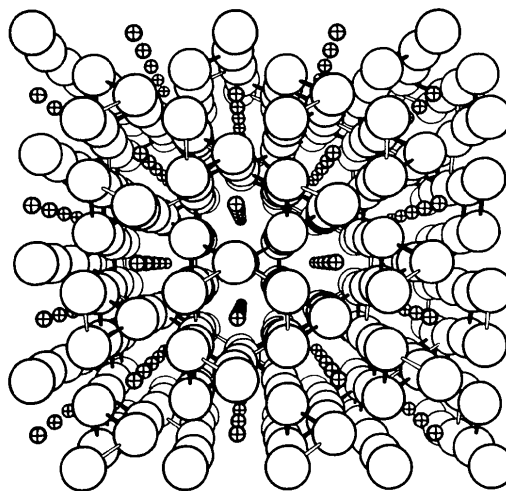


Fig. 2. The proposed structure of LiTe_3 viewed along the C axis with A_1 directed to the right in the plane of the paper. Te and Li atoms are drawn with arbitrary radii of 0.7 and 0.2 Å respectively. Nearest-neighbor intra-'chain' Te contacts are indicated by the same bond-shading scheme used in Fig. 1.

Table 5. The 36-fold general positions in R_4 space group for LiTe_3

(a) Four-dimensional

$$(0,0,0,0); (\frac{2}{3}, \frac{1}{3}, \frac{1}{3}, 0); (\frac{1}{3}, \frac{2}{3}, \frac{2}{3}, 0) +$$

x	y	z	ζ
$-y$	$x - y$	z	ζ
$-x + y$	$-x$	z	ζ
$-x$	$-y$	$-z$	$-\zeta$
y	$-x + y$	$-z$	$-\zeta$
$x - y$	x	$-z$	$-\zeta$
$-y$	$-x$	z	$\frac{1}{2} + \zeta$
$-x + y$	y	z	$\frac{1}{2} + \zeta$
x	$x - y$	z	$\frac{1}{2} + \zeta$
y	x	$-z$	$\frac{1}{2} - \zeta$
$x - y$	$-y$	$-z$	$\frac{1}{2} - \zeta$
$-x$	$-x + y$	$-z$	$\frac{1}{2} - \zeta$

(b) Three-dimensional

$$(0,0,0); (\frac{2}{3}, \frac{1}{3}, \frac{1}{3}); (\frac{1}{3}, \frac{2}{3}, \frac{2}{3}) + *$$

$\bar{x} + u(\tau)$	$\bar{y} + v(\tau)$	$\bar{z} + w(\tau)$
$-\bar{y} - v(\tau)$	$\bar{x} - \bar{y} + u(\tau) - v(\tau)$	$\bar{z} + w(\tau)$
$-\bar{x} + \bar{y} - u(\tau) + v(\tau)$	$-\bar{x} - u(\tau)$	$\bar{z} + w(\tau)$
$-\bar{x} - u(-\tau)$	$-\bar{y} - v(-\tau)$	$-\bar{z} - w(-\tau)$
$\bar{y} + v(-\tau)$	$-\bar{x} + \bar{y} - u(-\tau) + v(-\tau)$	$-\bar{z} - w(-\tau)$
$\bar{x} - \bar{y} + u(-\tau) - v(-\tau)$	$\bar{x} + u(-\tau)$	$-\bar{z} - w(-\tau)$
$-\bar{y} - v(\frac{1}{2} + \tau)$	$-\bar{x} - u(\frac{1}{2} + \tau)$	$\bar{z} + w(\frac{1}{2} + \tau)$
$-\bar{x} + \bar{y} - u(\frac{1}{2} + \tau) + v(\frac{1}{2} + \tau)$	$\bar{y} + v(\frac{1}{2} + \tau)$	$\bar{z} + w(\frac{1}{2} + \tau)$
$\bar{x} + u(\frac{1}{2} + \tau)$	$\bar{x} - \bar{y} + u(\frac{1}{2} + \tau) - v(\frac{1}{2} + \tau)$	$\bar{z} + w(\frac{1}{2} + \tau)$
$\bar{y} + v(\frac{1}{2} - \tau)$	$\bar{x} + u(\frac{1}{2} - \tau)$	$-\bar{z} - w(\frac{1}{2} - \tau)$
$\bar{x} - \bar{y} + u(\frac{1}{2} - \tau) - v(\frac{1}{2} - \tau)$	$-\bar{y} - v(\frac{1}{2} - \tau)$	$-\bar{z} - w(\frac{1}{2} - \tau)$
$-\bar{x} - u(\frac{1}{2} - \tau)$	$-\bar{x} + \bar{y} - u(\frac{1}{2} - \tau) + v(\frac{1}{2} - \tau)$	$-\bar{z} - w(\frac{1}{2} - \tau)$

* To be interpreted as $\bar{x} \rightarrow \bar{x} + \frac{2}{3}, \bar{y} \rightarrow \bar{y} + \frac{1}{3}, \bar{z} \rightarrow \bar{z} + \frac{1}{3}$, etc. Since, in general, $\tau = k_1x + k_2y + k_3z$, τ changes when a rhombohedral centering translation (or any other lattice translation) is added to the positions in this table.

ment with the observed data.* Te atom parameters corresponding to this value are listed in Table 3, grouped according to special positions in $P\bar{3}c1$.

Observed neutron diffraction data were compared with patterns each computed from the Te atom positions derived above and one of several possible sets of sites for Li atoms. Coherent scattering lengths of -0.214×10^{-12} and 0.543×10^{-12} cm were assumed for Li and Te respectively. Details of four models tested are given in Table 2. Agreement indices, defined as $\Sigma |I_{\text{obs}} - I_{\text{calc}}| / \Sigma I_{\text{obs}}$, demonstrate that model 1 is probably more correct than any of the other models tested. Li atom parameters from model 1, expressed as special positions in $P\bar{3}c1$, are included in Table 3.

Discussion

The proposed structure

The approximate atomic arrangement we suggest for LiTe_3 bears interesting similarities to the structure of elemental Te. The reference structure of LiTe_3 would correspond to a simple cubic lattice if Li atoms were replaced by Te. The actual trigonal structure of elemental Te could then be produced by regular atom displacements from this hypothetical lattice (Bradley, 1924). For LiTe_3 , displacements of Te atoms from their reference structure positions are parallel or antiparallel to the same basal-plane directions followed by the larger displacements (0.37 \AA in Te, up to 0.17 in LiTe_3) that conceptually convert 'cubic Te' to its actual structure.

Just as the 'displaced' atoms in elemental Te form infinite chains along triad axes, the sections of the proposed LiTe_3 structure where displacements are greatest contain segments of recognizable Te chains. Table 4 shows that the intra-chain bond distances and angles in these sections approach the values found for Te (2.87 \AA , 102.3° respectively; Bradley, 1924). Sections where displacements are least have the metal-like Te environments of the reference structure. Chain-like and metal-like sections alternate in sheets normal to C with a period of 5.34 \AA . Even in metal-like sections, each Te atom has two nearest Te neighbors, and 'infinite chains' can thus be traced parallel to the triad axes in LiTe_3 . The structure of one such 'chain' over a period of 26.7 \AA is shown in Fig 1(a); the manner in which two and three adjacent 'chains' entwine is indicated in Fig. 1(b) and (c).

The nested Te 'chains' leave channels centered on triad axes, along which Li atoms are regularly distri-

buted (see Fig. 2). Li environments in the reference structure are but little changed as a consequence of the displacements of Te atoms. Li-Te distances vary only from 3.08_2 \AA in sections where the Te configurations are most metal-like to 3.08_5 \AA in sections where the Te chains are most recognizable. (The Li-Te distance in Li_2Te is 2.82 \AA .)

Two unresolved questions relevant to this proposed structure concern (1) the unique axial ratio ($C/A = \sqrt{\frac{3}{8}}$) of the rhombohedrally centered hexagonal reference structure cell, and (2) the absence of a domain structure in single-crystal candidates. The latter may be explained by the likely existence of Te chains in the liquid phase that, on crystallization, direct one unique trigonal axis parallel to themselves. With this view, the description of the LiTe_3 structure in terms of displacements from a metal-like reference structure should be restated as displacements from an assembly of chains.

The suggested explanation of the second question does not illuminate the first, however. The persistence of $C/A = \sqrt{\frac{3}{8}}$ from -103 to 150°C becomes more unusual if linear rather than three-dimensionally equiaxed Te configurations are selected as a reference structure.

The utility of modulated symmetry arguments

We have described the approximate superstructure of LiTe_3 in terms of a simple first-order harmonic positional modulation of Te atoms because that model adequately represents the observed diffraction data as we have recorded them. We cannot claim that Fourier or least-squares refinement of the independently variable parameters in Table 3, using precise observed structure factors, would not modify this description in detail. However, in agreement with de Wolff (1974) we conclude that applications of modulated symmetry arguments may, especially in simple cases such as LiTe_3 , provide convenient shortcuts to the derivation of certain superstructures whose atomic parameters are related in special ways not apparent from their space group.

We are indebted to J. R. DiStefano who provided the purified and recast Li metal used in this work. We also thank J. W. Cable and H. G. Smith who recorded the neutron diffraction data and commented on their interpretation.

APPENDIX

The space group in R_4 that represents the proposed structure of LiTe_3 has the 36-fold general positions shown in Table 5 expressed (a) in terms of coordinates x , y , z and ζ (where ζ is the fractional coordinate along the R_4 basis vector that is perpendicular to

* Note the close limits within which U_c can be fixed, even though only qualitative local intensity comparisons are available. This is a consequence of sensitive dependences on U_c of relative intensities of satellites and their neighboring main reflections, and of intensities of main reflections not equivalent by virtue of the $\bar{3}m$ Laue symmetry.

R_3 space), and (b) in terms of coordinates \bar{x} , \bar{y} and \bar{z} and the functions $u(\tau)$, $v(\tau)$ and $w(\tau)$. The origin is chosen as a symmetry center in R_4 . A possible symbol for this group might be $R_{3v} \bar{3}^+e$.

References

- AALST, W. VAN, DEN HOLLANDER, J., PETERSE, W. J. A. M. & DE WOLFF, P. M. (1976). *Acta Cryst.* B32, 47–58.
- BRADLEY, A. J. (1924). *Phil. Mag.* 48, 447–496.
- CUNNINGHAM, P. T., JOHNSON, S. A. & CAIRNS, E. J. (1973). *J. Electrochem. Soc.* 120, 328–330.
- FOSTER, M. S., JOHNSON, C. E., DAVIS, K. A., PECK, J. & SCHABLASKE, R. (1969). USAEC Report ANL-7575, p. 141.
- JOHNSON, C. K. (1976). Private communication.
- WOLFF, P. M. DE (1974). *Acta Cryst.* A30, 777–785.
- WONDRATSCHEK, H., BÜLOW, R. & NEUBÜSER, J. (1971). *Acta Cryst.* A27, 523–535.
- ZINTL, E., HARDER, A. & DAUTH, B. (1934). *Z. Elektrochem.* 40, 588–593.

Acta Cryst. (1977). B33, 1396–1399

An X-ray Diffraction Study of Sodium Thiosulphate Pentahydrate, $\text{Na}_2\text{S}_2\text{O}_3 \cdot 5\text{H}_2\text{O}$

BY A. AYDIN URAZ† AND N. ARMAĞAN

University of Ankara Faculty of Science, Department of Physics, Beşevler, Ankara, Turkey

(Received 28 June 1976; accepted 24 October 1976)

A three-dimensional X-ray diffraction study of sodium thiosulphate pentahydrate was based on densitometer-measured photographic data. The structure was refined by full-matrix least squares to an R (excluding zero-weight data) of 0.082 for 1301 reflexions and an R (including zero-weight data) of 0.089 for 1359 reflexions. The Na–O distances range from 2.386 (6)–2.439 (7) Å for Na(1) octahedra and 2.331 (6)–2.418 (6) Å for Na(2) octahedra. In the tetrahedral $\text{S}_2\text{O}_3^{2-}$ anion the S–S and S–O bond lengths are 2.015 (3) and 1.455 (5)–1.490 (4) Å respectively. The hydrogen-bonding scheme described by previous workers is basically confirmed. The controversy over the O(8)–H(9) \cdots S(1*) bond seems to be clarified in this work.

Introduction

The crystal structure of sodium thiosulphate pentahydrate has been determined by Taylor & Beever (1952) using two-dimensional X-ray diffraction intensity data. El Saffar (1968) has reported the positional parameters of H atoms deduced from his NMR studies. Padmanabhan *et al.* (1971) refined the above-mentioned crystal structure from two-dimensional neutron diffraction data and they basically confirmed the hydrogen-bonding scheme as proposed by Taylor & Beever (1952) and El Saffar (1968), with the exception of atom H(9). Baur (1972) suggests that this disagreement needs clarification. Manojlović-Muir (1975) has claimed that the differences in bond distances in $\text{S}_2\text{O}_3^{2-}$ ions may be attributed to the thermal vibrations of the atoms in the ion.

In view of this, we have undertaken this three-dimensional work as part of a project in which the effects of the environment and thermal vibration on bonding in the $\text{S}_2\text{O}_3^{2-}$ ion in several ionic thiosulphates are being examined.

Experimental

A crystal of hexagonal prismatic habit was cut and ground into a cylinder 0.135 mm in diameter and 0.6 mm in length, so that the cylinder axis corresponded to the [100] axis. All the X-ray data were collected with this crystal.

Crystal data

$\text{Na}_2\text{S}_2\text{O}_3 \cdot 5\text{H}_2\text{O}$, FW 248.2. Monoclinic, space group $P2_1/c$, $a = 5.941$, $b = 21.570$, $c = 7.525$ Å, $\beta = 103^\circ 55'$, $Z = 4$ (Taylor & Beever, 1952; Padmanabhan *et al.*, 1971). The linear absorption coefficient for Cu $K\alpha$ radiation was found to be 59.7 cm^{-1} .

Intensity measurement

With Cu $K\alpha$ radiation and Weissenberg equi-inclination techniques, multiple-film exposures were taken of the layers $0 \leq h \leq 5$. The intensities of all the reflexions were measured photometrically with a Joyce–Loebl microdensitometer. Of the possible 1764 reflexions, 1359 were classified as observed, and about

† To whom correspondence should be addressed at: I. Cadde 89/4, Bahçelievler, Ankara, Turkey.